An automated method for adaptive radiation therapy for prostate cancer patients using continuous fiducial-based tracking

2010 Phys. Med. Biol. 55 65

(http://iopscience.iop.org/0031-9155/55/1/005)

IOP PUBLISHING PHYSICS IN MEDICINE AND BIOLOGY

Phys. Med. Biol. **55** (2010) 65–82 doi:10.1088/0031-9155/55/1/005

An automated method for adaptive radiation therapy for prostate cancer patients using continuous fiducial-based tracking

C E Noel, L Santanam, J R Olsen, K W Baker and P J Parikh[1]

Department of Radiation Oncology, Washington University School of Medicine, 4921 Parkview Place, St Louis, MO 63110, USA

E-mail: pparikh@radonc.wustl.edu

Received 20 July 2009, in final form 16 October 2009
Published 30 November 2009
Online at stacks.iop.org/PMB/55/65

Abstract

Electromagnetic tracking technology is primarily used for continuous prostate localization during radiotherapy, but offers potential value for evaluation of dosimetric coverage and adequacy of treatment for dynamic targets. We developed a highly automated method for daily computation of cumulative dosimetric effects of intra- and inter-fraction target motion for prostate cancer patients using fiducial-based electromagnetic tracking. A computer program utilizing real-time tracking data was written to (1) prospectively determine appropriate rotational/translational motion limits for patients treated with continuous isocenter localization; (2) retrospectively analyze dosimetric target coverage after daily treatment, and (3) visualize three-dimensional rotations and translations of the prostate with respect to the planned target volume and dose matrix. We present phantom testing and a patient case to validate and demonstrate the utility of this application. Gamma analysis of planar dose computed by our application demonstrated accuracy within 1%/1 mm. Dose computation of a patient treatment revealed high variation in minimum dose to the prostate (D_{min}) over 40 fractions and a drop in the D_{min} of ≈8% between a 5 mm and a 3 mm PTV margin plan. The infrastructure has been created for patient-specific treatment evaluation using continuous tracking data. This application can be used to increase confidence in treatment delivery to targets influenced by motion.

(Some figures in this article are in colour only in the electronic version)

1. Introduction

Dose escalation in radiation therapy of prostate cancer has been shown to improve disease-free survival and local control (Zelefsky *et al* 1998, Pollack *et al* 2002, Peeters *et al* 2006). With

[1] Author to whom any correspondence should be addressed.

the advancement of conformal radiation therapy techniques, planned dose delivery can be shaped to the target while limiting dose to nearby normal tissue and critical structures, such as the bladder and rectum (Dearnaley *et al* 1999). However, uncertainties in daily localization of the prostate have historically called for inclusion of excessive margins in the planning target volume (PTV) (Roach *et al* 1994). The involvement of increased toxicity to proximal organs limits further dose escalation to the target volume, including hypo-fractionation and partial prostatic boosts.

Several population-based methods have been proposed for determining treatment planning margins (Van Herk *et al* 2000, British Institute of Radiology 2003). Such methodologies incorporate common uncertainties introduced during radiation therapy, including inter- and intra-fraction organ motion, to define margins that provide acceptable coverage for 90% of patients. Still, standard use of margins determined from population-based criteria may lead to inadequate treatment for some patients and overtreatment for others.

Many studies reporting on the potential benefits gained from reduced PTV margins suggest that the degree of beneficence from margin reduction is patient specific and may be dependent upon the shape of the target and its proximity to nearby organs at risk (Yan *et al* 2001, Huang *et al* 2008, Gordon and Siebers 2009). Adaptive radiation therapy for the prostate using patient-specific margins and varying action levels based on inter-fraction set-up error has been published in detail (Yan *et al* 1995, 1997, De Boer and Heijmen 2001). More recently, an effort has been made to use volumetric imaging (cone-beam computed tomography (CBCT) or megavoltage computed tomography (MVCT)) for adaptive dose calculation (Woodford *et al* 2007, Lee *et al* 2008, Wu *et al* 2008). While reports of potential benefits utilizing an image-guided based method are promising, clinical implementation has been limited for several reasons (table 1).

Real-time electromagnetic tracking has recently been introduced into clinics for use of target localization, both before and during treatment. This technology utilizes continuous tracking to monitor the isocenter position. Studies assessing inter- and intra-fraction prostate motion have provided increased evidence that target displacement during treatment is not negligible and may be critical during treatment (Litzenberg *et al* 2006, Kupelian *et al* 2007, Hossain *et al* 2008, Langen *et al* 2008).

Continuous target tracking during treatment can be used to promote target coverage by signaling the therapist to hold beam delivery when the prostate exceeds certain motion boundaries. This technique can be highly effective for translational motion; however, prostate rotation is more difficult to manage since it can be independent of the external body and treatment couch. Several methods for online correction of rotational offsets have been proposed. The use of a treatment table with the ability to rotate is one option; however, this equipment is limited to small rotations, can introduce increased potential for table/gantry collisions and requires increased patient immobilization to prevent further organ displacement rotated under gravitational forces (Bel *et al* 2000, Guckenberger *et al* 2007). Advanced online correction strategies implemented through calculation of optimized collimator/gantry angles (Rijkhorst *et al* 2007), multi-leaf collimator shapes (Court *et al* 2005) and beam fluence deformation (Mohan *et al* 2005) have been detailed elsewhere, but these investigations have focused on pre-treatment patient set-up rather than intra-fraction motion compensation. While several studies have attempted to quantify the impact of rotations on dose delivery to the target using repeat imaging and simulations, incorporation of continuous intra-fraction rotation data has not yet been included in these dosimetric evaluations (Cranmer-Sargison *et al* 2008, Redpath *et al* 2008).

Although real-time tracking is designed to enable online intervention for correction of target misalignments, reported motion data can potentially be used for dosimetric evaluation

Table 1. Limitations of image-guided techniques for adaptive radiation therapy.

Limitations	References
(1) Regular QA and accuracy of HU units for dose computation	Oelfke *et al* (2006), Baumann *et al* (2008), Verellen (2008) and Mc Parland (2009)
(2) Mechanical limitations: limited FOV, isocentric/geometric uncertainties due to gantry sag	Oelfke *et al* (2006) and Verellen (2008)
(3) Image quality: increased noise and artifacts due to scatter, constraints on reconstruction algorithms, and blurring from organ motion	Oelfke *et al* (2006), Verellen (2008), Chen *et al* (2009), Mc Parland (2009) and Tran (2009)
(4) Only accounts for inter-fraction anatomical variability	Verellen (2008), Chen *et al* (2009)
(5) Equipment/technical costs	Baumann *et al* (2008), Mc Parland (2009) and Tran (2009)
(6) Staffing and user training (acquisition, registration, target delineation)	Baumann *et al* (2008), Chen *et al* (2009), Mc Parland (2009) and Tran (2009)
(7) Accuracy/reproducibility of automatic and manual soft-tissue delineation	Chen *et al* (2009), Mc Parland (2009) and Tran (2009)
(8) Accuracy of image registration techniques (manual and automatic)	Verellen (2008), Chen *et al* (2009) and Tran (2009)
(9) Additional patient dose	Moseley *et al* (2007), Murphy *et al* (2007), Verellen (2008), Mc Parland (2009) and Tran (2009)
(10) Data storage/transfer	Swerdloff (2007), Baumann *et al* (2008), Chen *et al* (2009) and Mc Parland (2009)
(11) Acquisition/reconstruction/registration time	Oelfke *et al* (2006), Baumann *et al* (2008), Verellen (2008), Chen *et al* (2009), Mc Parland (2009) and Tran (2009)

of delivered treatment. Additionally, it can enable establishment of motion tolerances prior to treatment. With pre-treatment knowledge of acceptable rotation limits for individual patients, adequacy of daily patient set-up can be easily assessed before treatment delivery occurs.

Use of this technology offers a new approach to the adaptive therapy process that bypasses many of the challenges involved in adaptive radiation therapy using volumetric imaging. To ensure optimal efficacy we established several requirements in the development of our dose evaluation method. First, target localization data used for daily patient set-up and subsequent plan evaluation should have high spatial accuracy. In order to provide positional target information comparable to that provided by current image-based localization techniques, positional uncertainty should be no larger than that given by fiducial-based imaging, a technique that has been established to yield accurate and consistent patient alignment (Dehnad *et al* 2003, Van Der Heide *et al* 2007). Second, the method must be cost-effective in resources. It should require minimal additional time on the part of the therapist, physicist, physician and

patient. It should be highly automated and objective in order to minimize time spent by clinical personnel and should provide an appropriate metric and easily defined acceptance/rejection criteria. Additionally, transfer and storage of data used for dose delivery evaluation should be fast and easy. Third, a visualization tool must be integrated to aid in clarification of target motion experienced before and during treatment and its relationship with the three-dimensional dose matrix. Finally, it should account for both inter- and intra-fraction target motion in six degrees of freedom (translations and rotations).

Using these guidelines, our goal was to utilize continuous localization data provided by electromagnetic tracking to evaluate dosimetric coverage of our prostate cancer patients. We developed a computer-based tool to (1) prospectively determine appropriate rotational and translational motion limits for prostate cancer patients treated with continuous isocenter localization, (2) retrospectively analyze dosimetric target coverage using tracked positions of individual patient data and (3) visualize both theoretical and actual three-dimensional rotations and translations of the prostate with respect to a stationary PTV and dose matrix. This application, referred to as SWIFTER (Semi-Automatic Workflow using Intra-fraction Fiducial-based Tracking for Evaluation of Radiotherapy), enables the assessment of potentially more effective treatment techniques that simultaneously introduce more risks, such as dose escalation, sub-prostatic boosts and reduced-margin treatment planning.

2. Materials and methods

2.1. Real-time tracking system

The Calypso® 4D Localization System (Calypso Medical Technologies, Inc., Seattle, WA) uses an electromagnetic array to track passive Beacon® electromagnetic transponders (8.5 × 1.85 mm glass-encapsulated copper coils) implanted in the patient's prostate. Implantation by general clinical protocol involves transrectal insertion of three transponders placed at the left base, right base and apex of the prostate. Implantation instructions provided with each Beacon® set recommend transponders to be placed equidistant from the center of the prostate and spaced 2 cm apart. The stability of these implanted transponders has been previously reported (Litzenberg *et al* 2007a). The three-dimensional coordinates of each transponder, with respect to treatment isocenter, are determined from the CT scan taken during simulation. These coordinates are entered into the Calypso System to serve as the planned treatment position. During localization on the treatment machine, the electromagnetic array, a rectangular panel encasing electromagnetic coils, is positioned over the patient's pelvis. The coils emit a radiofrequency signal to excite the implanted transponders. The transponders then return a signal at a specific frequency, allowing for their positions to be detected relative to the array at a nominal sampling rate of 10 Hz. The array (equipped with reflective surface markers) in turn is tracked by three infrared cameras mounted to the ceiling, providing absolute positional information of the transponders. The isocenter position as calculated from the transponder locations is tracked and reported throughout treatment. The system also monitors ambient radiation in the treatment room for synchronization with tracking data, enabling identification of target motion collected during active radiation delivery. Previous studies done by Balter *et al* (2005) and Parikh *et al* (2005) have documented the submillimeter accuracy of the system.

2.2. Tracking data

2.2.1. Prospective motion limits. The Calypso System is designed for both set-up localization and continuous monitoring of the isocenter position. At the time of initial localization, the Calypso System reports translational shifts and rotational offsets, as compared to the planned

transponder positions. The user is allowed to set patient-specific rotational limits for patient set-up. If the system detects prostate rotation greater than this value, the user is warned during initial localization.

Additionally, the user is allowed to set patient-specific motion limits of translational isocenter movement. The system is designed to warn the user if the isocenter exceeds these limits during treatment. Limits for each axis (lateral, anterior–posterior, and superior–inferior) are set independently, allowing for asymmetrical motion boundaries. Our method is designed to determine the appropriate rotational and translational motion limits for each patient, before treatment. This is done using a computer simulation that identifies the maximum rotation and translation the prostate can undergo before exceeding its PTV boundaries. The target structure is virtually moved through a set of theoretical rotations/translations and excursions of the displaced volume from the stationary PTV structure are detected in search of optimal motion boundaries. Details of this method are presented in section 2.4.1.

2.2.2. Retrospective dose analysis. Tracking data from each treatment fraction is stored by the Calypso System on the tracking station. The clinical system at our institution is equipped with supplementary functionality allowing for exportation of individual transponder positions to an external computer. Individual tracking files are exported into an Excel (Microsoft Corporation) spreadsheet via a non-clinical software application. This option is not standard on clinical systems and is designed for research purposes.

Data exported for each fraction consists of individual transponder and isocenter positions as a function of time. Also included is synchronized radiation detection data. Transponder positions are sampled and recorded sequentially at a nominal sampling frequency of 10 Hz, resulting in reported isocenter positions approximately every 0.1 s. This data is used to create a probability density histogram of target rotations and translations for convolution with the planned dose distribution.

2.3. Treatment planning system data

The patient plan is exported from the treatment planning system (TPS) into an external viewing application (Computational Environment for Radiotherapy Research (CERR), Washington University, St Louis, MO) (Deasy *et al* 2003). The CERR application is designed to import contours, beams, dose and images from both RTOG and DICOM formats for conversion into a common MATLAB (Mathworks, Natick, MA) data structure. This feature enables universal compatibility with any treatment planning system with RTOG or DICOM export functionality.

The prostate or clinical target volume (CTV) contours from CT simulation are extracted and used as the mobile target structure. The PTV structure is designated as the bounding structure which is used as a constraint on the CTV to determine appropriate motion limits. Alternately, a bounding structure could be generated from an isodose line to form a dose rind in order to constrain the target structure to a dose boundary. The three-dimensional dose array is used for dose computation. Multiple treatment prescriptions are supported to accommodate treatment plans that include two treatment volumes, which are common for intermediate and high-risk prostate patients.

2.4. The SWIFTER application

A MATLAB (vR2006b) computer program was written to process and analyze treatment plan and Calypso tracking data. This application automatically extracts information from the plan

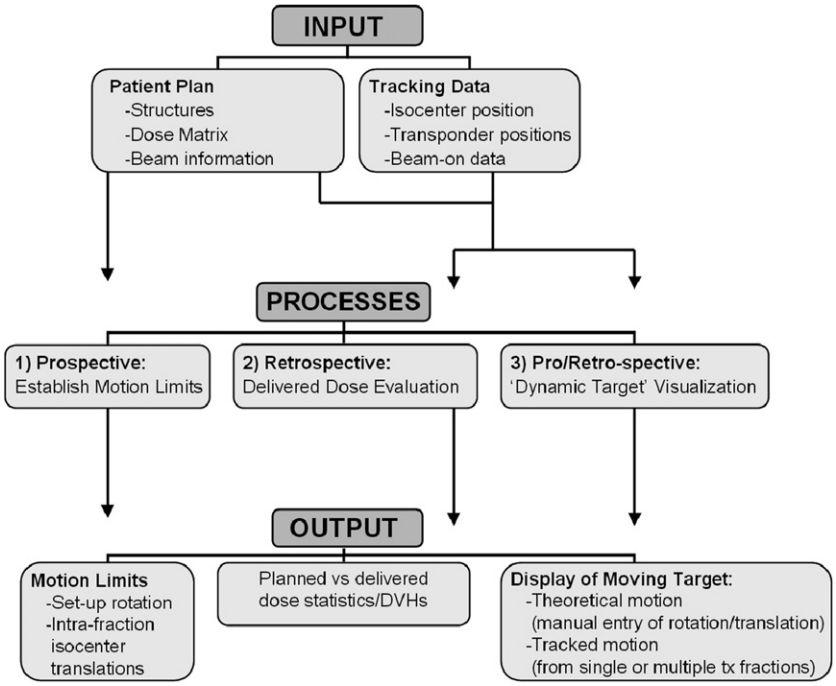

Figure 1. Flowchart of input data, application processes and output data.

to register the structures, dose and absolute transponder data in the treatment room reference frame. The data flow and functionalities are summarized in figure 1.

2.4.1. Prospectively determining patient-specific motion tolerances. First, prospective motion limits can be established. Rotational set-up tolerances are assessed by virtually moving the structure through a series of theoretical rotations and translations. A binary approach is used to judge appropriateness of rotational limits. When the target structure is detected as exceeding the bounding structure's volume, the motion condition is flagged. Because real-time target rotations are not reported during treatment and therefore are not used as criteria by which intra-fraction radiation delivery is held, the SWIFTER application is programmed to assume set-up rotation as a systematic offset when testing translational motion limits. By testing translational and rotational limits concurrently, SWIFTER is able to detect conditions where an intra-fraction translation or rotation might push the prostate out of the PTV. An example of such a condition is shown in figure 2. Consequently, patient-specific translational tolerances that compensate for geometric misalignments caused by prostate rotations during treatment are established by SWIFTER.

These translational motion limits are also assessed by binary pass/fail criteria. SWIFTER identifies conditions when the target structure exceeds PTV boundaries. Since there is no way of directly controlling intra-fraction rotation during treatment, the application attempts to reduce translational motion limits before reducing rotational limits in efforts to minimize the volume of the target outside the bounding structure. Several PTV margins can be tested (e.g. 3 mm, 5 mm, 8 mm) to decide on the most appropriate one to encompass theoretical rotations.

A set of theoretical rotations encompassing a range of common rotations observed during patient treatment was established from a dataset of inter- and intra-fraction prostate rotations.

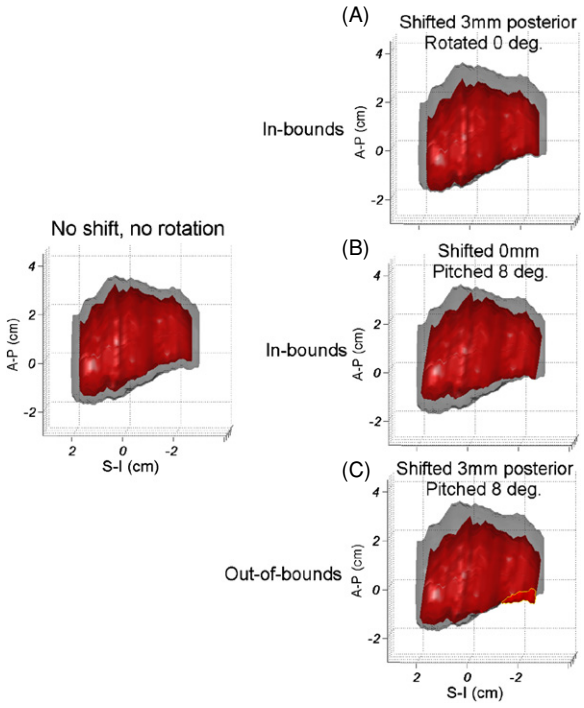

Figure 2. Example of a condition where a combination of rotational and translational motion would push the prostate (red structure) out of a 3 mm PTV margin (gray structure): (A) prostate is within the PTV for a 3 mm shift (no rotation); (B) prostate is within the PTV for 8° rotation (no shift); (C) prostate falls out of the PTV when rotated 8° and shifted 3 mm. SWIFTER tests all three cases to detect such conditions.

Approximately 30 h of tracking data collected from a group of ten prostate cancer patients was analyzed. A range limited within two standard deviations of the mean of rotations about each axis (lateral, superior–inferior (S–I) and anterior–posterior (A–P)) was established. Figure 3 displays a frequency histogram of this dataset.

An upper translational motion tolerance of 3 mm (coinciding with tolerances used for a multi-institutional clinical Calypso study (Kupelian *et al* 2007) and a lower tolerance of 2 mm (the minimal allowed setting by the Calypso System) was used for translational motion limit testing. SWIFTER is designed to test combinations in a hierarchical fashion for optimum speed. Large rotations, which are more likely to fail than smaller rotations, are tested first. If the rotation fails, the program ceases testing further translational combinations and continues with the next smallest rotational value.

2.4.2. Retrospectively estimating delivered dose. Next, SWIFTER is designed to perform dose computation using real-time patient tracking data to estimate dose delivered to the target during treatment. Dose computation could potentially be performed after each treatment fraction. SWIFTER is designed to allow for combination of previous analysis with the 'dose of the day' to provide accumulated dosimetric effects. Consequently, the delivered dose distribution can be monitored throughout treatment to detect poor plan efficacy before a large dosimetric impact is incurred (figure 4).

Tracking data exported from the system is applied to the target structure. Translational motion of the isocenter is reported by the Calypso System, however explicit rotation data is

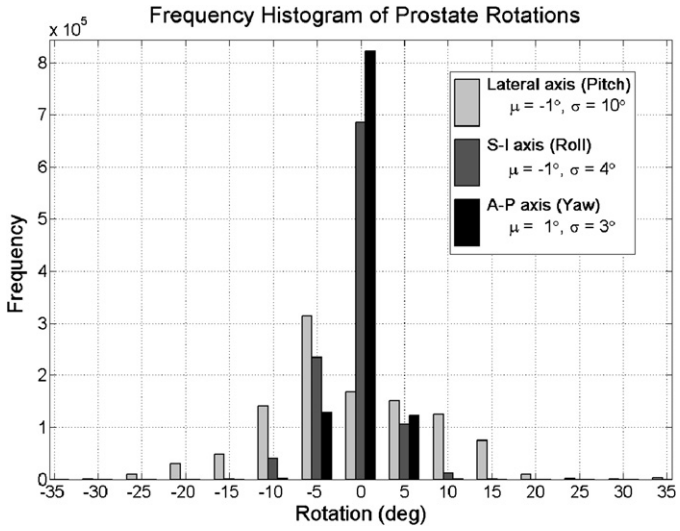

Figure 3. Frequency histogram of inter- and intra-fraction prostate rotations (difference from planned position) about the lateral, S–I and A–P axes.

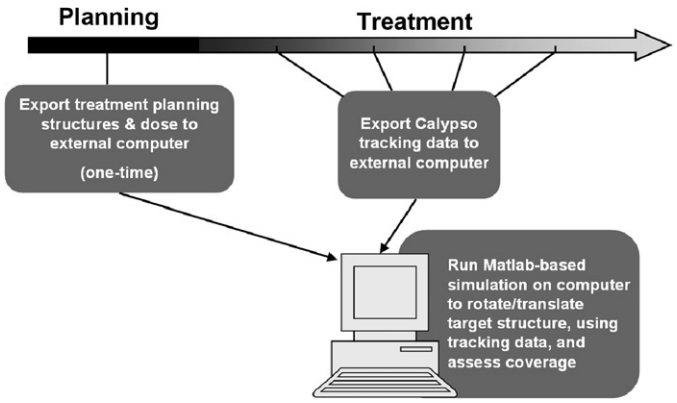

Figure 4. Workflow for retrospective dose analysis.

not. Rigid rotations are calculated by SWIFTER by minimizing the fiducial registration error using a least-squares method. Three-dimensional rotations and translations with resolutions of 1° and 0.05 cm, respectively, are binned into a six-dimensional frequency histogram.

The three-dimensional target volume is then virtually rotated and translated within the static dose cloud to each position differentiated by the frequency bins. Thus, for each distinct rotation/translation, every voxel comprising the target structure is displaced to a new location inside the three-dimensional dose array. At each position (bin), the dose to every voxel is recorded and mathematically weighted by the frequency of that positional occurrence. The end product is a matrix of indexed voxels and their accumulated doses, as determined by the amount of time spent at different locations within the dose array. The target structure alone is treated as a dynamic volume, while the rigid body (skin) and surrounding structures are assumed to be static structures.

As tracking data is added daily to SWIFTER for each individual patient, previous results are combined with new analysis in order to calculate cumulative dose to each voxel. Statistics and dose volume histograms (DVHs) are computed on the planned and delivered dose distributions to evaluate the adequacy of the plan under real target motion.

2.4.3. Visualizing target motion. Finally, SWIFTER allows for visualization of the target structure with respect to the stationary PTV and three-dimensional dose array. The visualization tool allows the user to manually enter rotations and translations to display the displaced prostate relative to the treatment room reference frame. Additionally, processed tracking data can be input for visualization of target motion collected during treatment. Sequential positions from tracked data can be read in as a function of time to simulate actual movement of the target under radiation delivery. Processed tracking data can also be read as a frequency table of each target position and the amount of target volume exceeding the PTV. In this manner, the user can visualize the actual prostate positions as a function of occurrence frequency or percentage of volume excursion. This visualization tool can be used to ensure that the rotations and translations measured by the Calypso System are physiologic and do not represent corrupted or flawed data.

2.5. Phantom study

A phantom study was conducted to validate the process in its entirety (including data transfer, coordinate transformation, calculation of rotations, dose analysis, etc). The accuracy of dose computation for a structure under the influence of rotational and translational offsets was tested using controlled phantom tracking data and a patient treatment plan.

The data (structure set, plan information and dose matrix) from a seven-field intensity-modulated radiation therapy (IMRT) prostate treatment plan was exported from the Pinnacle treatment planning system (TPS) (v8.0 m, Philips Medical Systems, Madison, WI) into the SWIFTER application. To ensure the accuracy of SWIFTER's dose computation in both high and low-dose areas and over high gradient regions of the dose distribution, we performed testing with a structure encompassing a larger area of the treatment volume (as opposed to simply the high-dose target area surrounding the prostate). For this reason, the skin contour was designated as the dynamic target structure for dose computation.

Tracking data was obtained using a $10 \times 10 \times 13$ cm^3 cubic phantom (QA Fixture—Calypso® Medical Technologies, Inc., Seattle, WA) embedded with three Calypso transponders. The phantom was imaged on the Philips Brilliance 64-slice CT scanner (Philips Medical Systems) with 1.5 mm slice thickness, and the image set was transferred to the Pinnacle TPS. The isocenter position (identified from external marks on the phantom surface) and transponder locations obtained from CT images were entered into the Calypso System and the phantom was localized and tracked on the treatment machine. The phantom was translated ± 1 cm from the isocenter to offsets in the S–I, lateral and A–P directions and each position was separately tracked (six tracking sessions in total). The phantom was then re-aligned to the isocenter and tracking was repeated while the phantom was rotated $\pm 20^\circ$ (verified with a digital level) about each axis using a Styrofoam wedge. In total, tracking sessions were collected for 13 different positions: 0 cm/0° (no shift), ± 1 cm/0° along each axis (six total) and 0 cm/$\pm 20^\circ$ about each axis (six total). Transponder data was exported from the Calypso System for input into the SWIFTER application, and the resulting dose theoretically delivered to the skin contour was computed for each tracking session.

For three-dimensional evaluation of the accuracy of the SWIFTER application, axial, sagittal and coronal isocentric dose planes (1 mm dose grid spacing) were exported from the

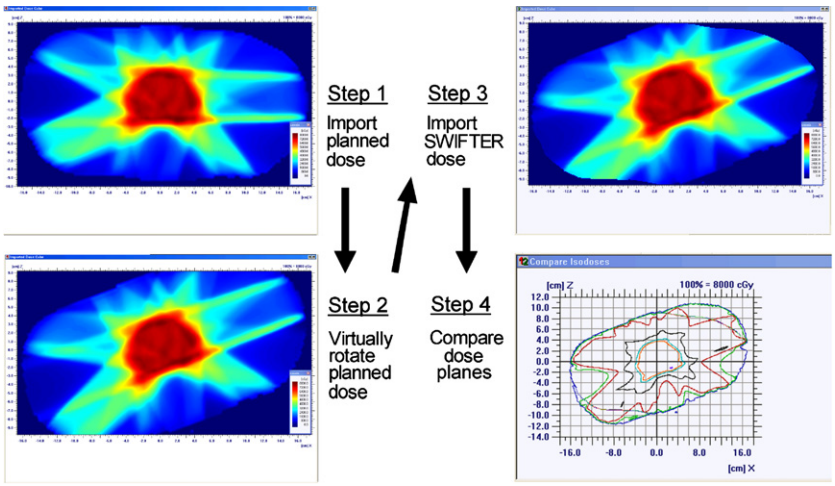

Figure 5. Screenshots from the commercial QA software showing the validation process by isodose comparison of axial dose planes (20° rotation) between the TPS and SWIFTER. Step 1: import the dose plane from the TPS into the commercial QA software; step 2: virtually rotate the planned dose plane 20° using the commercial QA software; step 3: import the dose plane analyzed by SWIFTER into the commercial QA software; step 4: compare dose planes between SWIFTER and the TPS (rotated). An overlay of isodose lines is shown.

TPS and SWIFTER to a commercial quality assurance (QA) analysis software (OmniPro-I′mRT v1.6, IBA Dosimetry, Germany). Each translated or rotated dose plane exported from our application was compared to the static dose plane (from the TPS), which was virtually translated/rotated by ± 1 cm/$\pm 20^\circ$ using the OmniPro-I′mRT software application. A set of screenshots taken from the commercial QA software is shown in figure 5 to provide an example of this method. Planes were analyzed using the Gamma method (tolerance of 1 mm/1%) and computation of per cent dose difference inside a region of interest defined by the skin contour.

2.6. Patient case study

The data from a prostate cancer patient treated with a standard seven-field IMRT plan using a 5 mm margin PTV was acquired for analysis. A total dose of 75.6 Gy at an energy of 18 MV was planned for delivery over 42 fractions. Contouring and planning was done on a CT dataset with 1.5 mm slice thickness using the Pinnacle TPS. A magnetic resonance (MR) image acquired before transponder implantation was used to supplement prostate delineation.

Real-time tracking data using a 3 mm action limit for beamhold (in any individual direction) was acquired from the patient's treatment to assess actual dose delivery. Since the tracking data used for this case study includes intra-fraction beam-hold interventions, it is likely that the dosimetric impact of prostate motion is less severe than for a case including no intervention. Tracking data was unavailable for two treatment sessions, so analysis was completed using the remaining 40 fractions. Inter-fractional and cumulative dose computation was performed (using only 'beam-on' motion data), and planned and delivered dose distributions were compared. Maximum dose (D_{max}), minimum dose (D_{min}), mean dose (D_{mean}) and percent of prescription dose covering 95% of the prostate volume (D_{95}) were calculated and used as a metric to assess the coverage and homogeneity of the delivered dose

Table 2. Per cent dose difference between dose planes exported from the SWIFTER application ($Dose_{SWIFTER}$) and the TPS ($Dose_{TPS}$). Viewing convention for orientation of rotation (clockwise (cw) or counterclockwise (ccw)) in the axial, sagittal and coronal planes is defined as view from feet, view from left and view from above, respectively.

Analyzed dose plane	Shift	Per cent dose difference $(Dose_{SWIFTER} - Dose_{TPS})/Dose_{TPS}$	
		Mean (%)	Standard deviation (%)
Axial	None	0.2	1.0
	+1 cm (left)	0.2	0.9
	−1 cm (right)	0.2	0.9
	+20° (cw)	0.4	1.9
	−20° (ccw)	0.4	1.7
Sagittal	None	0.8	1.7
	+1 cm (ant.)	0.8	1.7
	−1 cm (post.)	0.8	1.7
	+20° (ccw)	0.8	2.0
	−20° (cw)	0.8	2.0
Coronal	None	0.3	1.7
	+1 cm (sup.)	0.3	1.7
	−1 cm (inf.)	0.3	1.7
	+20° (ccw)	0.9	2.0
	−20° (cw)	0.9	2.0

distribution. A plan using a reduced PTV margin of 3 mm was generated for additional comparison, and dose computation was repeated using patient tracking data. Planned D_{max}, D_{min}, D_{mean} and D_{95} for each plan (as expressed in percentages) were comparable at 108.7, 99.6, 102.7 and 100.8 for the 5 mm margin treatment plan and 109.9, 99.8, 102.5 and 100.9 for the 3 mm margin treatment plan. The time required for each step in the dose evaluation process was recorded to assess the time efficiency of our technique.

3. Results

3.1. Phantom study

Gamma analysis revealed over 99% of dose points in each plane processed by SWIFTER agreed to within 1 mm/1% of dose planes exported from the TPS. The average point-by-point percent difference for all planes was <1%, with a maximum standard deviation of 2%. The mean percentage difference and standard deviation for each analyzed plane are reported in table 2.

3.2. Patient case study

The transfer of patient plan data (dose, plan, structures) from the TPS to an external computer in MATLAB-based format required approximately $10\frac{1}{2}$ min. The determination of appropriate rotational and translational motion limits was reported within seconds. Processing Calypso tracking data for a single fraction (including exportation of tracking data, importation into a MATLAB-based format, data sampling, calculation of rotations and distribution of

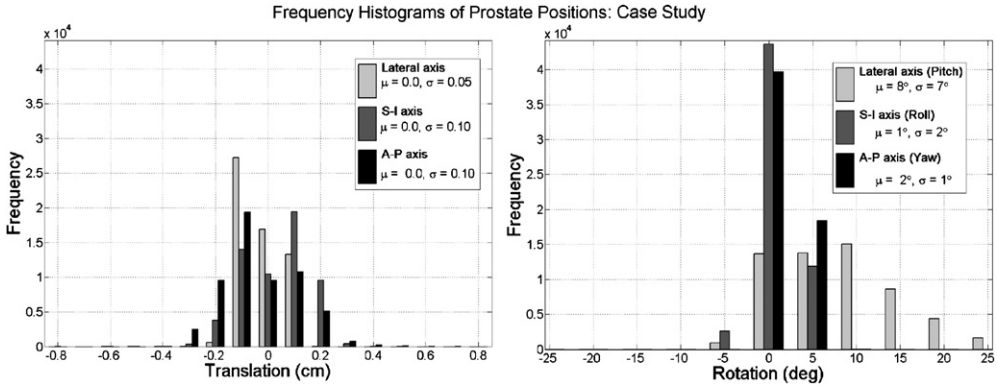

Figure 6. Frequency histogram of inter- and intra-fraction prostate translations (left) and rotations (right) for patient case. Only 'beam-on' data is reported.

Table 3. Approximate time requirement for each process in the SWIFTER application (on a per-fraction basis). The shaded process indicates a task performed only once. The approximate total time for cumulative dose computation of 40 fractions is 80 min.

Frequency	Process	Sub-processes	Time	
Per patient (one-time)	Transfer of patient plan data	Export patient RTOG plan, dose and structures	$\frac{1}{2}$ min	10 $\frac{1}{2}$ min
		Import plan data into CERR/MATLAB	10 min	
Per tx fraction	Transfer and processing of patient tracking data	Export Calypso tracking	(seconds)	7–10 min
		Import into Excel	1 min	
		Read Excel, process	$\frac{1}{4}$ min	
		Bin positions	3$\frac{1}{2}$ min	
	Dose computation and analysis	Dose computation	2–5 min	
		Generation of dose statistics	(seconds)	

positions into frequency bins) required approximately 5 min. On average, an additional 2–5 min was required to complete dose computation for each individual fraction. This value varied depending on the number of positional bins. Table 3 displays each process and its associated time requirement for dose evaluation of a treatment single fraction. Cumulative dose computation for 40 fractions was completed in 80 min.

The average translational position of the isocenter during radiation delivery (while the treatment beam was on) was 0.0 cm in the lateral, S–I and A–P directions. The range of motion for each axis was −0.6 to 0.2 cm, −0.8 to 0.5 cm and −0.4 to 0.7 cm, respectively. Rotational motion during radiation delivery was largest around the lateral axis (pitch), with a mean of 8° and a range of −7° to 27°. This trend has been reported in several other studies (Dehnad *et al* 2003, Van Der Heide *et al* 2007) and is most likely due to bladder and rectum filling. The average rotations around the S–I and A–P axes (roll and yaw, respectively) were within 2° (figure 6).

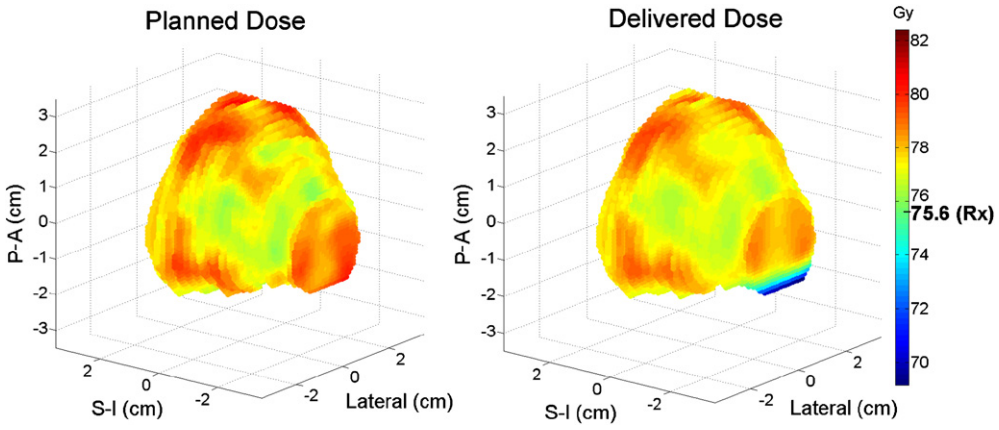

Figure 7. Three-dimensional representation of the prostate structure surface and planned (left) and delivered (right) dose distribution for the 3 mm margin plan. The prescription dose (75.6 Gy) is indicated on the colorbar.

Table 4. Cumulative dose statistics (planned and delivered) for the prostate for both 5 mm PTV and 3 mm PTV IMRT treatment plans. Values are represented as percentages of the prescribed dose.

	5 mm PTV margin			3 mm PTV margin		
Metric	Delivered (% of Rx)	Planned (% of Rx)	Difference (delivered–planned)	Delivered (% of Rx)	Planned (% of Rx)	Difference (delivered–planned)
D_{max}	106.5	108.7	−2.2	106.9	109.0	−2.1
D_{min}	98.7	99.6	−0.9	91.5	99.8	−8.3
D_{mean}	102.7	102.7	0.0	102.5	102.5	0.0
D_{95}	101.3	100.8	0.5	101.0	100.9	0.1

The delivered D_{max}, D_{min}, D_{mean} and D_{95} to the prostate expressed as percentages of the prescription dose were 106.5%, 98.7%, 102.7% and 101.3% (respectively) for the 5 mm PTV plan. These values agreed to within 2.2% of the planned dose statistics. The delivered D_{max}, D_{min}, D_{mean} and D_{95} values for the 3 mm PTV plan were generally similar at 106.9%, 91.5%, 102.5% and 101.0%, respectively. All values for the 3 mm PTV plan, with the exception of D_{min}, were within 2.1% of the planned dose statistics. The delivered D_{min} was 8.3% lower than the planned D_{min}. Figure 7 displays a three-dimensional representation of the prostate volume and the planned and delivered dose to the target. A concentration of low-dose voxels is found at the posterior portion of the prostate apex for the delivered dose distribution, indicating that part of the volume was not adequately covered. Cumulative dose results are tabulated in table 4.

Computation of dose statistics for individual treatment fractions revealed increased inter-fraction instability of D_{max} and D_{min} as compared to D_{95} (figure 8), particularly for the 3 mm PTV plan. D_{min} experienced the greatest instability across all treatment fractions with a standard deviation of 8.0% for the 5 mm PTV plan and 12.2% for the 3 mm PTV plan (table 5).

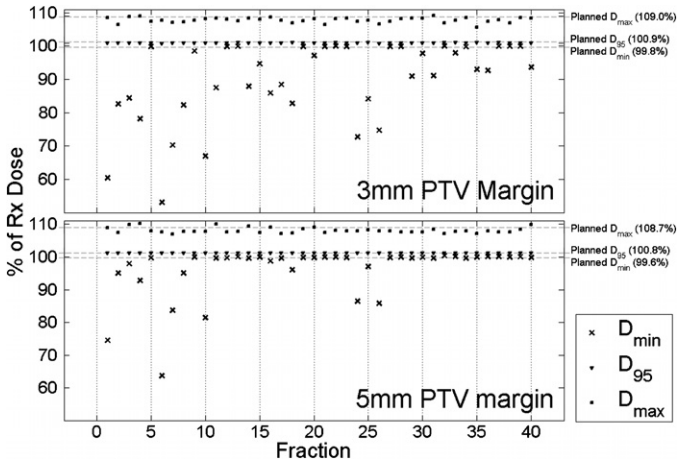

Figure 8. $D_{\min}$, $D_{\max}$ and D_{95} of the prostate for each individual treatment for the 3 mm margin (top) plan and 5 mm margin (bottom) plan. Dose values are expressed as a percentage of the prescription dose.

Table 5. Mean and standard deviation of dose statistics over 40 fractions (planned and delivered) for the prostate for both 5 mm PTV and 3 mm PTV IMRT treatment plans.

	5 mm PTV margin		3 mm PTV margin	
Metric	Mean (%)	Standard deviation (%)	Mean (%)	Standard deviation (%)
$D_{\max}$	108.0	0.8	107.8	0.8
$D_{\min}$	96.2	8.0	89.7	12.2
D_{mean}	102.7	<0.0	102.5	0.1
D_{95}	101.2	<0.0	100.9	0.1

4. Discussion and conclusion

The development of methods to mitigate uncertainties presented by daily target localization is ongoing. Evaluation of target coverage from daily dose delivery can provide increased certainty in treatment efficacy and help enable adaptive planning decisions. This can be demonstrated by the patient case study presented here. Computation of cumulative dose delivery indicated a considerable drop in the minimum dose to the prostate from a 5 mm to 3 mm PTV margin treatment plan. While potentially adequate coverage might be offered by the 5 mm PTV margin treatment plan over a 40-fraction treatment course, it is important to consider the effect of a hypo-fractionated treatment scheme for such a patient. For example, the variability observed in the $D_{\min}$ over the first ten fractions indicates a possible under-dosing to the prostate during the beginning of treatment. This would cause an exaggerated effect of a hypo-fractionated treatment scheme. It should be taken under consideration that the dosimetric effects presented in this patient case include intra-fraction beam-hold intervention. Dose computation of an intervention-free treatment might have revealed a larger dosimetric miss. Incorporation of daily target coverage review would help enable an inter-fraction intervention before a large dosimetric impact is incurred.

There are several possible approaches for achieving daily evaluation of dose delivery, such as the fiducial-based method we have described here or image-guided based methods described elsewhere (Woodford *et al* 2007, Lee *et al* 2008, Wu *et al* 2008); however each technique carries different limitations.

Fiducial-based methods entail an invasive implantation procedure. By contrast, daily image guidance for use as a medium for pre-treatment set-up and adaptive radiation therapy is noninvasive. Although the invasive nature of fiducial implantation is a drawback, the procedure has become routine at many clinics and poses little additional health risk to the patient (Shinohara and Roach 2008, Linden *et al* 2009).

An important consideration is that fiducial-based localization may not be sensitive to volumetric organ deformation and does not report direct position data for neighboring organs. This limits our knowledge of shape variation of the prostate and dosimetric impact on normal tissues. As compared with fiducial-based techniques, image-guided techniques can provide a substantial amount of information about the position and geometry of the target and nearby tissues. Still, a study done by Van Der Wielen *et al* (2008) found that deformation of the prostate with respect to intraprostatic fiducials was small. Additionally, Deurloo *et al* (2005) reported that the magnitude of prostate deformation is secondary compared with organ motion and intra-observer variability in target delineation. While fiducial-based methods provide limited knowledge of the daily dosimetric impact on normal tissues, analytical efforts are focused on target anatomy in the high-dose region. The large amount of data provided by volumetric imaging entail that additional efforts are not required for a fiducial-based technique.

There are several reasons why clinical implementation of volumetric imaging as a means of adaptive radiation therapy is still challenging. Dosimetric computation based on volumetric imaging requires fast and accurate image segmentation. Since soft tissue is often not as clearly defined on CBCT and MVCT as bony anatomy or implanted fiducials, definition of target borders is subject to inter-observer variability (Song *et al* 2006, Moseley *et al* 2007, White *et al* 2009). Studies comparing localization based on soft-tissue segmentation to localization based on imaged fiducials provide evidence of increased uncertainty in determination of patient shifts during treatment set-up. Moseley *et al* (2007) compared soft-tissue-based localization shifts to fiducial-based localization shifts for 15 prostate cancer patients with implanted fiducial markers. Soft-tissue localization was done using CBCT images, while fiducial-based localization was done using orthogonal imaging of the fiducial markers, which was considered the gold standard. Localization shifts agreed to within 3 mm over 99% of the time in the lateral direction, but less than 75% of the time in both anterior–posterior and superior–inferior directions. Similar findings have also been reported in patients who undergo helical megavoltage imaging (Langen *et al* 2005). The time required for an observer to define the target and approve the 'dose of the day' can be costly, both for the observer and the patient. Automatic segmentation methods are under development but are currently limited.

Daily imaging and dose re-calculation generates large quantities of imaging, structure and dose information. The time and space required to transfer and store this information are considerable. In an article detailing the data management issues involved in image-guided radiation therapy, Swerdloff (2007) estimated that one image-guided radiation therapy session would require 150 MB of computer storage. By comparison, the amount of data generated by real-time tracking data for the entire course of treatment is less than 100 MB. Accordingly, data transfer speed is also faster.

Image-guided radiation therapy also delivers a considerable amount of dose to the patient. While daily imaging sessions can increase patient dose anywhere from 1.5 to 8cGy per day (Moseley *et al* 2007, Murphy *et al* 2007), real-time electromagnetic tracking contributes no additional radiation dose.

One of the most significant advantages of utilizing continuous tracking data for dose delivery evaluation is the incorporation of intra-fraction motion. Adaptive radiation therapy techniques using volumetric imaging alone must rely on the condition that the internal anatomy remains stationary between the time of image acquisition and the end of treatment. It is well documented that the prostate can experience intra-fraction movement ranging from several millimeters to a few centimeters (Litzenberg *et al* 2006, Kupelian *et al* 2007, Hossain *et al* 2008, Langen *et al* 2008). While use of online imaging to assess intra-fraction prostate motion has been reported by many studies (Kotte *et al* 2007, Boda-Heggemann *et al* 2008, Hossain *et al* 2008), we found in a previous investigation that pre- and post-treatment imaging and intermittent imaging may not accurately reflect prostate motion during treatment, even with a high sampling rate (Noel *et al* 2009).

With current limitations on image-guided adaptive radiation therapy, a fiducial-based method like the one described here may be advantageous. Further development of this tool could improve its utility. First, incorporation of biomechanical models of the prostate, bladder and rectum could enable prediction of adjoining structures in the high-dose region. Also, real-time beam and multi-leaf collimator information acquired from treatment could be used in place of a static dose cloud, as has been shown by Litzenberg *et al* (2007b).

Future advancements might make real-time fiducial-based dose evaluation a possible method for other anatomical targets impacted by intra-fraction motion, such as lung and abdomen tumors. The magnitude of motion and degree of tissue deformation of these targets elevates the complexity of estimating dose delivery. The application of the method described here for thoracic targets would require the development of different anatomic models, but may be a potential technique as the field of adaptive radiation therapy advances. For current clinical use as a dose delivery evaluation tool for prostate cancer patients, our fiducial-based method can provide increased confidence for radiation treatment.

References

Balter J M, Wright J N, Newell L J, Friemel B, Dimmer S, Cheng Y, Wong J, Vertatschitsch E and Mate T P 2005 Accuracy of a wireless localization system for radiotherapy *Int. J. Radiat. Oncol. Biol. Phys.* **61** 933–7

Baumann M, Hölscher T and Zips D 2008 The future of IGRT—cost benefit analysis *Acta Oncol.* **47** 1188–92

Bel A, Petrascu O, Van De Vondel I, Coppens L, Linthout N, Verellen D and Storme G 2000 A computerized remote table control for fast on-line patient repositioning: implementation and clinical feasibility *Med. Phys.* **27** 354–8

Boda-Heggemann J, Köhler F M, Wertz H, Ehmann M, Hermann B, Riesenacker N, Küpper B, Lohr F and Wenz F 2008 Intrafraction motion of the prostate during an IMRT session: a fiducial-based 3D measurement with cone-beam CT *Radiat. Oncol.* **3** 37

British Institute of Radiology 2003 *Geometric Uncertainties in Radiotherapy: Defining the Planning Target Volume* (London: BIR Publications)

Chen G T Y, Sharp G C and Mori S 2009 A review of image-guided radiotherapy *Radiol. Phys. Technol.* **2** 1–12

Court L E, Dong L, Lee A K, Cheung R, Bonnen M D, O'Daniel J, Wang H, Mohan R and Kuban D 2005 An automatic CT-guided adaptive radiation therapy technique by online modification of multileaf collimator leaf positions for prostate cancer *Int. J. Radiat. Oncol. Biol. Phys.* **62** 154–63

Cranmer-Sargison G 2008 A treatment planning investigation into the dosimetric effects of systematic prostate patient rotational set-up errors *Med. Dosim.* **33** 199–205

Dearnaley D P, Khoo V S, Norman A R, Meyer L, Nahum A, Tait D, Yarnold J and Horwich A 1999 Comparison of radiation side-effects of conformal and conventional radiotherapy in prostate cancer: a randomised trial *Lancet* **353** 267–72

Deasy J O, Blanco A I and Clark V H 2003 CERR: a computational environment for radiotherapy research *Med. Phys.* **30** 979–85

De Boer H C J and Heijmen B J M 2001 A protocol for the reduction of systematic patient setup errors with minimal portal imaging workload *Int. J. Radiat. Oncol. Biol. Phys.* **50** 1350–65

Dehnad H, Nederveen A J, Van Der Heide U A, Van Moorselaar R J A, Hofman P and Lagendijk J J W 2003 Clinical feasibility study for the use of implanted gold seeds in the prostate as reliable positioning markers during megavoltage irradiation *Radiother. Oncol.* **67** 295–302

Deurloo K E I, Steenbakkers R J H M, Zijp L J, De Bois J A, Nowak P J C M, Rasch C R N and Van Herk M 2005 Quantification of shape variation of prostate and seminal vesicles during external beam radiotherapy *Int. J. Radiat. Oncol. Biol. Phys.* **61** 228–38

Gordon J J and Siebers J V 2009 Coverage-based treatment planning: optimizing the IMRT PTV to meet a CTV coverage criterion *Med. Phys.* **36** 961–73

Guckenberger M, Meyer J, Wilbert J, Baier K, Sauer O and Flentje M 2007 Precision of image-guided radiotherapy (IGRT) in six degrees of freedom and limitations in clinical practice *Strahlenther Onkol.* **183** 307–13

Hossain S, Xia P, Chuang C, Verhey L, Gottschalk A R, Mu G and Ma L 2008 Simulated real time image guided intrafraction tracking-delivery for hypofractionated prostate *IMRT Med. Phys.* **35** 4041–8

Huang S H, Catton C, Jezioranski J, Bayley A, Rose S and Rosewall T 2008 The effect of changing technique, dose, and PTV margin on therapeutic ratio during prostate radiotherapy *Int. J. Radiat. Oncol. Biol. Phys.* **71** 1057–64

Kotte A N T J, Hofman P, Lagendijk J J W, van Vulpen M and Van Der Heide U A 2007 Intrafraction motion of the prostate during external-beam radiation therapy: analysis of 427 patients with implanted fiducial markers *Int. J. Radiat. Oncol. Biol. Phys.* **69** 419–25

Kupelian P *et al* 2007 Multi-institutional clinical experience with the Calypso System in localization and continuous, real-time monitoring of the prostate gland during external radiotherapy *Int. J. Radiat. Oncol. Biol. Phys.* **67** 1088–98

Langen K M, Lu W, Ngwa W, Willoughby T R, Chauhan B, Meeks S L, Kupelian P A and Olivera G 2008 Correlation between dosimetric effect and intrafraction motion during prostate treatments delivered with helical tomotherapy *Phys. Med. Biol.* **53** 7073–86

Langen K M, Zhang Y, Andrews R D, Hurley M E, Meeks S L, Poole D O, Willoughby T R and Kupelian P A 2005 Initial experience with megavoltage (MV) CT guidance for daily prostate alignments *Int. J. Radiat. Oncol. Biol. Phys.* **62** 1517–24

Lee L, Le Q and Xing L 2008 Retrospective IMRT dose reconstruction based on cone-beam CT and MLC log-file *Int. J. Radiat. Oncol. Biol. Phys.* **70** 634–44

Linden R A, Weiner P R, Gomella L G, Dicker A P, Suh D B, Trabulsi E J and Valicenti R K 2009 Technique of outpatient placement of intraprostatic fiducial markers before external beam radiotherapy *Urology* **73** 881–6

Litzenberg D W, Balter J M, Hadley S W, Sandler H M, Willoughby T R, Kupelian P A and Levine L 2006 Influence of intrafraction motion on margins for prostate radiotherapy *Int. J. Radiat. Oncol. Biol. Phys.* **65** 548–53

Litzenberg D W *et al* 2007a Positional stability of electromagnetic transponders used for prostate localization and continuous, real-time tracking *Int. J. Radiat. Oncol. Biol. Phys.* **68** 1199–206

Litzenberg D W, Hadley S W, Tyagi N, Balter J M, Ten Haken R K and Chetty I J 2007b Synchronized dynamic dose reconstruction *Med. Phys.* **34** 91–102

Mc Parland N A 2009 kV-cone beam CT as an IGRT tool in the treatment of early stage prostate cancer: a literature review *J. Med. Imaging Radiat. Sci.* **40** 9–14

Mohan R, Zhang X, Wang H, Kang Y, Wang X, Liu H, Ang K K, Kuban D and Dong L 2005 Use of deformed intensity distributions for on-line modification of image-guided IMRT to account for interfractional anatomic changes *Int. J. Radiat. Oncol. Biol. Phys.* **61** 1258–66

Moseley D J *et al* 2007 Comparison of localization performance with implanted fiducial markers and cone-beam computed tomography for on-line image-guided radiotherapy of the prostate *Int. J. Radiat. Oncol. Biol. Phys.* **67** 942–53

Murphy M J *et al* 2007 The management of imaging dose during image-guided radiotherapy: report of the AAPM Task Group 75 *Med. Phys.* **34** 4041–63

Noel C, Parikh P J, Roy M, Kupelian P, Mahadevan A, Weinstein G, Enke C, Flores N, Beyer D and Levine L 2009 Prediction of intrafraction prostate motion: accuracy of pre- and post-treatment imaging and intermittent imaging *Int. J. Radiat. Oncol. Biol. Phys.* **73** 692–8

Oelfke U, Tücking T, Nill S, Seeber A, Hesse B, Huber P and Thilmann C 2006 Linac-integrated kV-cone beam CT: technical features and first applications *Med. Dosim.* **31** 62–70

Parikh P J, Hubenschmidt J P, Dimmer S, Vertatschitsch E, Eidens R, Wright J N and Low D A 2005 4D verification of real-time accuracy of the Calypso system with lung cancer patient trajectory data *Int. J. Radiat. Oncol. Biol. Phys.* **63** S26–7

Peeters S T H, Heemsbergen W D, Koper P C M, Van Putten W L J, Slot A, Dielwart M F H, Bonfrer J M G, Incrocci L and Lebesque J V 2006 Dose-response in radiotherapy for localized prostate cancer: results of the Dutch multicenter randomized phase III trial comparing 68 Gy of radiotherapy with 78 Gy *J. Clin. Oncol.* **24** 1990–6

Pollack A, Zagars G K, Starkschall G, Antolak J A, Lee J J, Huang E, Von Eschenbach A C, Kuban D A and Rosen I 2002 Prostate cancer radiation dose response: results of the M D Anderson phase III randomized trial *Int. J. Radiat. Oncol. Biol. Phys.* **53** 1097–105

Redpath A T, Wright P and Muren L P 2008 The contribution of on-line correction for rotational organ motion in image-guided radiotherapy of the bladder and prostate *Acta Oncol.* **47** 1367–72

Rijkhorst E, Van Herk M, Lebesque J V and Sonke J 2007 Strategy for online correction of rotational organ motion for intensity-modulated radiotherapy of prostate cancer *Int. J. Radiat. Oncol. Biol. Phys.* **69** 1608–17

Roach M III , Pickett B, Rosenthal S A, Verhey L and Phillips T L 1994 Defining treatment margins for six field conformal irradiation of localized prostate cancer *Int. J. Radiat. Oncol. Biol. Phys.* **28** 267–75

Shinohara K and Roach M III 2008 Technique for implantation of fiducial markers in the prostate *Urology* **71** 196–200

Song W Y, Chiu B, Bauman G S, Lock M, Rodrigues G, Ash R, Lewis C, Fenster A, Battista J J and Van Dyk J 2006 Prostate contouring uncertainty in megavoltage computed tomography images acquired with a helical tomotherapy unit during image-guided radiation therapy *Int. J. Radiat. Oncol. Biol. Phys.* **65** 595–607

Swerdloff S J 2007 Data handling in radiation therapy in the age of image-guided radiation therapy *Semin. Radiat. Oncol.* **17** 287–92

Tran W T 2009 Practical considerations in cone beam and ultrasound IGRT systems in prostate localization: a review of the literature *J. Med. Imaging Radiat. Sci.* **40** 3–8

Van Der Heide U A, Kotte A N T J, Dehnad H, Hofman P, Lagenijk J J W and van Vulpen M 2007 Analysis of fiducial marker-based position verification in the external beam radiotherapy of patients with prostate cancer *Radiother. Oncol.* **82** 38–45

Van Der Wielen G J, Mutanga T F, Incrocci L, Kirkels W J, Vasquez Osorio E M, Hoogeman M S, Heijmen B J M and de Boer H C J 2008 Deformation of prostate and seminal vesicles relative to intraprostatic fiducial markers *Int. J. Radiat. Oncol. Biol. Phys.* **72** 1604–11.e3

Van Herk M, Remeijer P, Rasch C and Lebesque J V 2000 The probability of correct target dosage: dose-population histograms for deriving treatment margins in radiotherapy *Int. J. Radiat. Oncol. Biol. Phys.* **47** 1121–35

Verellen D, De Ridder M, Tournel K, Duchateau M, Reynders T, Gevaert T, Linthout N and Storme G 2008 An overview of volumetric imaging technologies and their quality assurance for IGRT *Acta Oncol.* **47** 1271–8

White E A, Brock K K, Jaffray D A and Catton C N 2009 Inter-observer variability of prostate delineation on cone beam computerised tomography images *Clin. Oncol.* **21** 32–8

Woodford C, Yartsev S, Dar A R, Bauman G and Van Dyk J 2007 Adaptive radiotherapy planning on decreasing gross tumor volumes as seen on megavoltage computed tomography images *Int. J. Radiat. Oncol. Biol. Phys.* **69** 1316–22

Wu Q J, Thongphiew D, Wang Z, Mathayomchan B, Chankong V, Yoo S, Lee W R and Yin F 2008 On-line re-optimization of prostate IMRT plans for adaptive radiation therapy *Phys. Med. Biol.* **53** 673–91

Yan D, Wong J, Vicini F, Michalski J, Pan C, Frazier A, Horwitz E and Martinez A 1997 Adaptive modification of treatment planning to minimize the deleterious effects of treatment setup errors *Int. J. Radiat. Oncol. Biol. Phys.* **38** 197–206

Yan D, Wong J W, Gustafson G and Martinez A 1995 A new model for 'accept or reject' strategies in off-line and on-line megavoltage treatment evaluation *Int. J. Radiat. Oncol. Biol. Phys.* **31** 943–52

Yan D, Xu B, Lockman D, Kota K, Brabbins D S, Wong J and Martinez A A 2001 The influence of interpatient and intrapatient rectum variation on external beam treatment of prostate cancer *Int. J. Radiat. Oncol. Biol. Phys.* **51** 1111–9

Zelefsky M J, Leibel S A, Gaudin P B, Kutcher G J, Fleshner N E, Venkatramen E S, Reuter V E, Fair W R, Ling C C and Fuks Z 1998 Dose escalation with three-dimensional conformal radiation therapy affects the outcome in prostate cancer *Int. J. Radiat. Oncol. Biol. Phys.* **41** 491–500